Experimental investigation on the CO$_2$ transcritical power cycle

CrossMark

Lisheng Pan[*], Bo Li[**], Xiaolin Wei[***], Teng Li

State Key Laboratory of High-temperature Gas Dynamics, Institute of Mechanics, Chinese Academy of Sciences, Beijing 100190, China

ABSTRACT

CO$_2$ has perfect environmental properties and has great potential to become a very ideal working fluid for power cycle. In the laboratory, a CO$_2$ transcritical power cycle system was established, using a rolling piston expander. Experimental study was carried out on the operating parameters, the electric power generated and the thermal efficiency. The pump operating speed and the load resistance were used to regulate the operating parameters. The results showed that there was a sudden decrease for the electric power generated in the start-up process. The electric power rose with increasing the converter frequency. When the converter frequency kept constant, the electric current declined with increasing the load resistance. In the experimental study, the steady electric power generated could reach about 1100 W and the thermal efficiency 5.0% when the high pressure was about 11 MPa and the low pressure was about 4.6 MPa. Though the isentropic efficiency, about 21.4%, was unsatisfactory, it still has important significance for the study on CO$_2$ expander.

© 2015 Elsevier Ltd. All rights reserved.

1. Introduction

The reserve of the low-grade heat energy is very huge, nevertheless the conventional power cycle technology is inefficient in exploiting or recovering this type energy. It is well known that power cycle with unconventional working fluid has good prospect in using low-grade heat energy. Researchers pay attention to two kind unconventional working fluids, namely, organic fluid and inorganic fluid. The ORC (organic Rankine cycle)) which uses the organic matter as working fluid attracts widely attention. It has distinct advantage in using low-grade heat energy. The potential organic fluid includes HCFCs (hydrochlorofluorocarbons), HFCs (hydrofluorocarbons) and HCs (hydrocarbons). Researchers carried out lots of work on optimizing the cycle conditions, selecting the optimal organic working fluids and improving the analysis method.

By the theoretical study on 20 fluids for ORC, Tchanche et al. [1] pointed out that HFC134a is the most suitable fluid for small scale ORC system with solar energy as heat source. Economic objective function was proposed for ORC in order to provide a basis for optimizing working fluid in account of the pay and the achievements [2]. The efficiency of the turbine or the expander usually keeps constant for different working fluids and conditions in theoretical study while it is impossible in practical project. Pan et al. [3] improved the theoretical analysis method of ORC based on radial flow turbine and gave performance of several fluids for ORC using 90 °C hot water as heat source. Pan et al. [4] also analyzed the regulation method for ORC power generation experimental system. CO$_2$ and NH$_3$ are the representatives of the inorganic fluid. CO$_2$ is an environment friendly and safe matter. Its basic thermal properties and environment properties are shown in Table 1. CO$_2$ is a waste product in many industry processes, thus the manufacturing cost is very lower than the organic fluids. The production of CO$_2$ is even too large, which causes that CCS (carbon dioxide capture and storage) technology has to be carried out in order to mitigate greenhouse effect [6–8]. Guo et al. [9] provided a comparison between the CO$_2$ transcritical power cycle and the R245fa Rankine cycle. Chen et al. [10] studied on the performance of transcritical power cycle with CO$_2$ and R32 as working fluid, respectively. Zeotropic mixtures which are composed of CO$_2$ and HCs are also studied for transcritical power cycle [11,12]. Zhang et al. [13,14] established a CO$_2$ transcritical power cycle system driven by solar energy and obtained the power generation efficiency of

M g/mol	t_b °C	t_c °C	p_c MPa	LFL %	ASHRAE 34 safety group	Atmospheric life yr	ODP /	GWP 100 yr
44.01	−78.4	31.0	7.38	none	A1	>50	0.00	1

8.78−9.45%. Kim et al. [15] carried out research on CO_2 transcritical power cycle and CO_2 supercritical power cycle with low-grade and high-grade heat energy as heat source. CO_2 supercritical power cycle is also well known as CO_2 supercritical Brayton cycle. In CO_2 supercritical Brayton cycle, CO_2 releasing heat energy at super-critical state, which differs from CO_2 transcritical power cycle. Batet et al. [16] established a model for CO_2 power cycle in using nuclear power and analyzed the performance in stable condition and variable condition. Garg et al. [17] compared the performance between CO_2 transcritical power cycle and steam transcritical power cycle. Split-flow recompression Brayton cycle is usually used to reduce the heat releasing to the environment and achieves a good temperature match between the heat transfer media [18]. Halimi et al. [19] studied the impact of reheating on the split-flow recompression Brayton cycle and pointed out that the reheating enhanced the thermal efficiency by 0.69%.

The investigation on CO_2 power cycle is significant for the development of the energy utilization efficiency in the future. However, the study on this type cycle is far from enough, especially experimental study. The high operating pressure and the difficulty in designing and manufacturing the expander or turbine are still hindering the experimental study. A CO_2 transcritical power cycle system is established in the laboratory. This article focuses on its performance and provides its operational aspect. The experience may be very useful for the following study on the CO_2 power cycle.

2. Methodology

2.1. The CO_2 transcritical power cycle system

CO_2 transcritical power cycle is a positive cycle. Usually, CO_2 has very large superheat degree at the expander exit in the cycle. In order to acquire high thermal efficiency, a regenerator is used to recover some heat energy of the fluid. The cycle using regenerator has six processes, namely, the expansion process in the expander, cooling process in the regenerator, the cooling and condensing process in the condenser, the pumping process in the pump, the heating process also in the regenerator, and the heating process in the supercritical heater, as shown in Fig. 1a. Accordingly, the system is mainly comprised of the expander, the regenerator, the condenser, the pump and the supercritical heater, as shown in Fig. 1b. A vapor liquid separator is also included to ensure that only liquid CO_2 flows into the fluid pump because of the harm from the vapor to the running pump.

There is also a thermal oil loop and a cooling water loop in the system. The thermal oil loop which includes an electric heater and an oil pump provides the heat source for the CO_2 transcritical power cycle system, while the cooling water offers the cold source. The system uses a refrigeration unit to produce cooling water instead of a cooling tower on account of the CO_2's low critical temperature. Temperature of the cooling water can be specified in the range from 0 °C to 30 °C. Because water will begin to freeze when its temperature reaches 0 °C, cooling water temperature in the experimental study keeps about 5 °C. If lower cold source is needed, water has to be replaced by other heat transfer medium
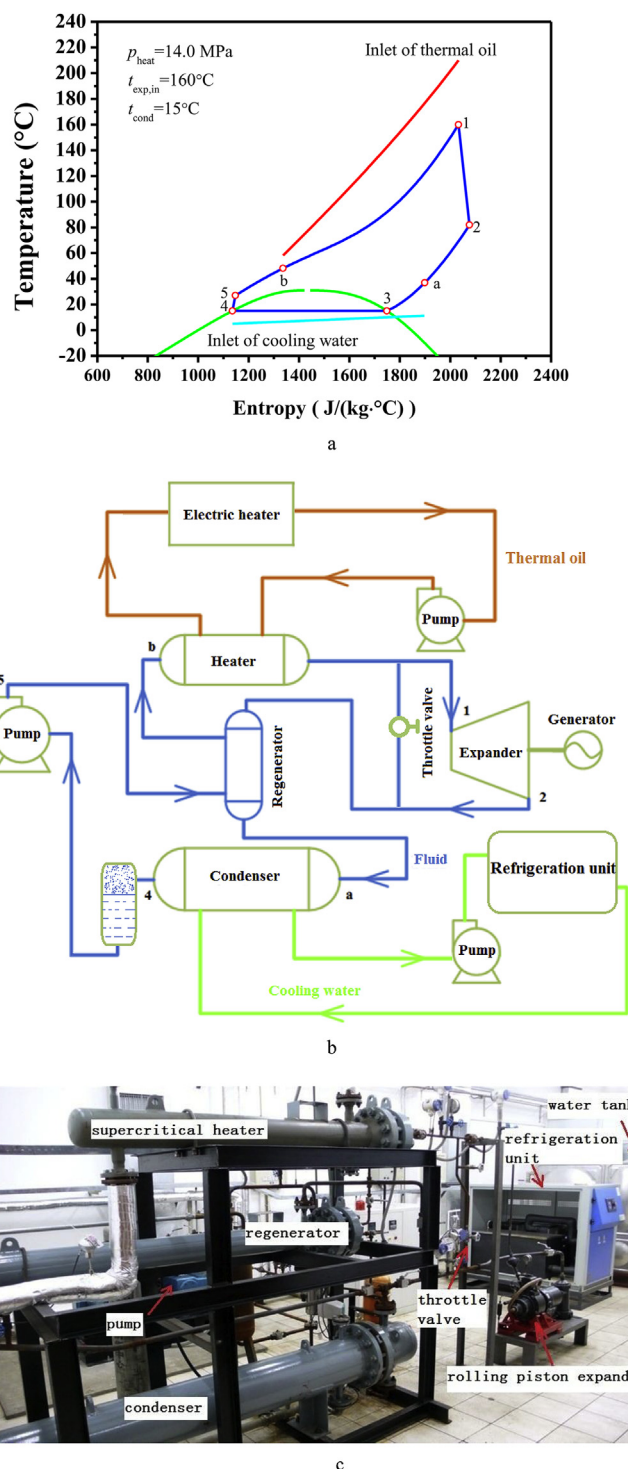

Fig. 1. a. T−s diagram for the CO_2 transcritical power cycle. b. Flow chart for the CO_2 transcritical power cycle system. c. The CO_2 transcritical power cycle system in laboratory.

like ethylene glycol aqueous solution. The system in kind is shown in Fig. 1c.

A 2.0 kW scale rolling piston expander is installed in the system. As shown in Fig. 2, there is an expansion cavity enclosed by the cylinder shell internal surface, the rolling piston surface and the glide board surface. The fluid expands in the cavity and drives the rolling piston and the main shaft until the fluid flows out from the expander outlet. The expander has a dead center. When the rolling piston is at the dead center, the working fluid can't start it. Therefore, an external force is needed in the start-up process. The special generator fixed in the expander shell can solve the problem. In the start-up process, the generator is used as an engine which can drive the expander away from the dead center with inputting electric power. When the expander starts successfully, the start-up mode should be turned to the operation mode immediately and the electric power can be generated.

Electric power is generated by the built-in three-phase permanent magnet generator whose axis is connected with the expander axis by a shaft coupling. Incandescent bulbs are used to consume the electric energy. Because it is a three-phase generator, three column bulbs are arranged in the bulb box as three load resistances. The series connection method is used to connect the bulbs in each column. Every bulb has one switch to control the connection or not. The delta connection method is used to connect the generator and the three load resistances. Each column is comprised of one 500 W bulb, one 200 W bulb, two 150 W bulbs, one 100 W bulb, one 60 W bulb and two 25 W bulbs. The bulb number of each column can be regulated by the switch fixed for each bulb. The rated voltage of the bulbs is all 220 V. The effect of the incandescent bulbs can be considered as pure resistance and their resistance values in rated condition are shown in Table 2. In order to make the generator and the expander operate smoothly, the three load resistances must have similar resistance value.
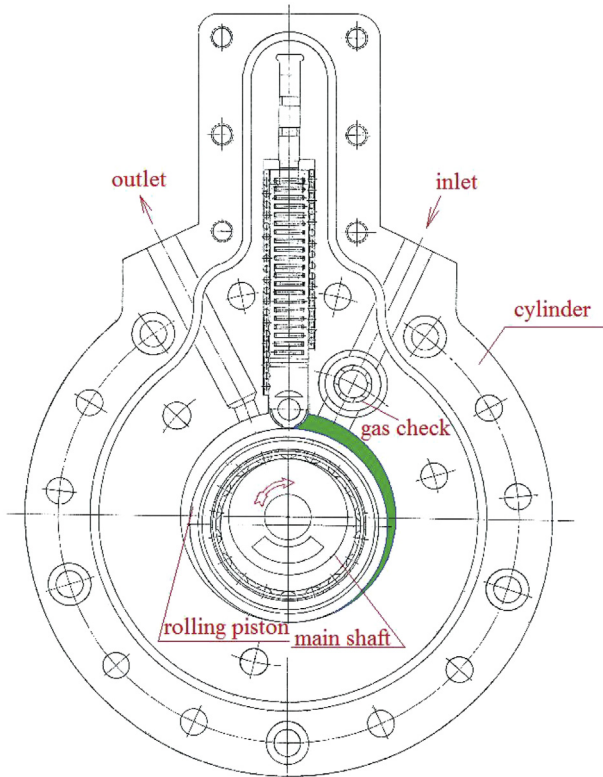

Fig. 2. The structure diagram of the rolling piston expander.

Table 2
The resistance values of the incandescent bulbs.

Rated power	W	500	200	150	100	60	25
Resistance values	Ω	96.8	242.0	322.7	484.0	806.7	1936.0

Detailed information of the instruments and the devices in the system is shown in Table 3. It needs to be pointed out that the supercritical heater in the system has less area than the optimization. This is the reason why the thermal oil temperature is very high while the CO_2 has low temperature in the exit of the supercritical heater. Therefore, the thermal efficiency and the generator effect can't reach the best result.

2.2. The uncertainty of the experimental data

Temperature is measured by the K-type temperature transmitters whose accuracy is ±0.5% (±1.0 °C). The pressure transmitters are used to get the pressure values in the system and can give an accuracy of ±0.5% (±0.05 MPa). The data acquisition and processing system has 12 bit precision. The accuracy of the mass flowmeter and the power meter are shown Table 3.

2.3. Definition of the performance parameters

In the system, CO_2 is heated in the supercritical heater by the thermal oil. Heat capacity in the heater can be expressed as Eq. (1). Enthalpy value at the entrance and the exit of the heater is achieved by referring to REFPROP 9.0 [20] according to the pressure and temperature. Mass flow rate of CO_2 is measured by the coriolis mass flowmeter. In theoretical study on power cycle performance, thermal efficiency is usually defined as the ratio of net power output to heat capacity in the evaporator or heater. However, in small scale experimental system, actual capacity of the equipments usually can't match each other perfectly. In particular, actual efficiencies of the expander and the pump are usually very low. Therefore, the fluid pump usually consumes electric power as much as that generated by the system. Thus thermal efficiency which is defined by the conventional method becomes meaningless in experimental study on small scale power cycle system. In this article, thermal efficiency is expressed as the ratio of electric power generated to heat capacity in the heater, as shown in Eq. (2). Electric power generated by the system is measured by the power meter.

$$\dot{Q}_{\text{heater}} = \left(h''_{\text{heater}} - h'_{\text{heater}} \right) \cdot \dot{m}_{CO_2} = (h_1 - h_b) \cdot \dot{m}_{CO_2} \qquad (1)$$

$$\eta_{\text{ther}} = \frac{\dot{P}_{\text{ge}}}{\dot{Q}_{\text{heater}}} \qquad (2)$$

Isentropic efficiency of the expander is defined as the ratio of enthalpy drop in the expander to isentropic enthalpy drop and is expressed as Eq. (3). Mechanical energy is produced by the expander and converted into electric energy by the generator. Energy loss exists in the transmission and generation process. Hence the actual efficiency of the expander-generator is lower than the expander isentropic efficiency. Enthalpy in the two equations is also obtained according to the data base REFPROP 9.0 and the state point parameters.

$$\eta_{\text{exp,isen}} = \frac{h'_{\text{exp}} - h''_{\text{exp}}}{h'_{\text{exp}} - h''_{\text{exp,isen}}} = \frac{h_1 - h_2}{h_1 - h_{2,\text{isen}}} \qquad (3)$$

Table 3
The information of instruments and measuring devices.

Item	Information
Supercritical heater	A shell and tube heat exchanger is used as supercritical heater in the CO_2 transcritical power cycle system. CO_2 flows in the tube pass while thermal oil in the shell pass. The design pressure for tube pass is 20 MPa in the tube pass. The heat exchange area is 1.19 m^2.
Regenerator	A shell and tube heat exchanger is used as regenerator in the system. Supercritical pressure CO_2 flows in the tube pass while subcritical pressure CO_2 in the shell pass. The design pressure for tube pass is also 20 MPa in the tube pass. The heat exchange area is 1.59 m^2.
Condenser	A shell and tube heat exchanger is used as condensor in the system. CO_2 flows in the tube pass while cooling water in the shell pass. The design pressure for tube pass is 8.0 MPa in the tube pass. The heat exchange area is 8.09 m^2.
Pump	A plunger pump is used to transport liquid CO_2 in the system. The model number is SJ4-M-630/2.5. The rated flow is 0.4 m^3/h. The rated inlet pressure is 2.0 MPa and the rated outlet pressure is 20 MPa. Its rotational speed can be controlled by a frequency converter which is connected with it.
Expander	A rolling piston expander is used in the system. The rated power is 2.0 kW and the rated rotational speed is 1000 rpm.
Generator	It is a three-phase permanent magnet generator. The rated rotational speed is 1000 rpm. The rated power and the rated voltage are 2.0 kW and 220 V (AC), respectively. It is fixed in the expander shell in order to achieve good sealing effect.
Refrigeration unit	The refrigeration unit can provide cooling water with temperature in the range from 0 °C to 30 °C. The control accuracy is ±1 °C. The refrigerating capacity is 34 kW as providing 5 °C cooling water.
Mass flowmeter	Coriolis mass flowmeter is used in the system. The model number is SITRANS F C MASSFLOW MASS2100 DI 15. The measuring range is 0–5600 kg/h and the accuracy is 0.1%. Working pressure is 0–12.8 MPa.
Power meter	Model number of the digital power meter used in the experiment is WT230. Measuring range of voltage is 0–600 V and measuring range of electric current is 0–20 A. Applicable frequency range is 0 and 0.5–100 kHz. The basic accuracy is 0.1%.

3. Results and discussion

3.1. Analysis of the start-up process

The start-up process of the system is as follows. Firstly, the throttle valve is used to throttle the working fluid and the parameters are adjusted to the start-up process according to Table 4. Secondly, the rolling piston of the expander is driven away from the dead center with the start-up mode and meanwhile CO_2 expands in the expander instead of throttle valve by regulating valves. Finally, the working fluid starts the expander and the start-up mode must be changed to the operation mode immediately. Then, electric power is generated by the system and is consumed by the incandescent bulbs.

In the start-up process, the expander inlet pressure is about 16 MPa and the inlet temperature is about 130 °C. Nevertheless, in the operation process, the expander inlet pressure is about 11 MPa and the inlet temperature is about 80 °C. High pressure difference and temperature difference leads to high enthalpy difference and high electric power generated. Consequently, the electric power generated can reach nearly 1700 W in the start-up process and declines rapidly, as shown in Fig. 3. Finally, the electric power generated keeps about 1000 W, as shown in Figs. 3 and 4. There is a trough for electric power generated in the transition from the start-up process to the operation process, which is caused by the abrupt change of the pressure difference and temperature difference.

3.2. Influence of the pump operating speed

In this experimental system, a plunger pump connected with a frequency converter is used to transport liquid CO_2. The frequency converter is used to regulate the cycle operation parameters, as well as the pump operating speed. The pressure difference provided by the pump is consumed by the pressure drop in the expander and the pressure drop in the heat exchangers and the tubes. This section gives the influence of the pump operating speed on the operating parameters. In this section, the temperature of the cooling water

Table 4
The parameters for the start-up process.

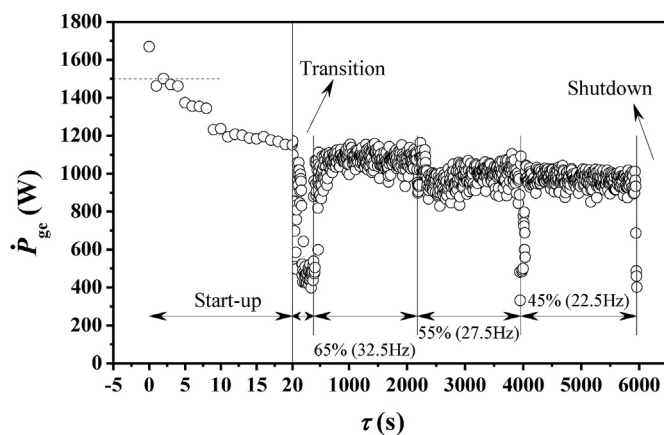| p'_{exp} MPa	t'_{exp} °C	p''_{exp} MPa	t_{cond} °C	t'_{oil} °C	$t'_{cooling}$ °C
16	130	4.5	10	210	5

Fig. 3. Variation of the electric power generated with time.

keeps about 5 °C and the thermal oil keeps about 210 °C. The condensing temperature is about 12.6 °C while the condensing pressure is about 4.7 MPa. The electric power generated is consumed by three 500 W bulbs.

As shown in Fig. 5, the expander inlet pressure decreases with decreasing the converter frequency and the pressure drop in the expander is about 6.5 MPa. The expander used in the system has higher flow capacity than the throttle valve. In the start-up process, the high pressure fluid flows rapidly into the expander immediately as turning on the expander pass and turning off the throttle valve pass suddenly. Consequently, the expander inlet pressure declines quickly and reaches a stable value in the start-up and the transition process. The converter frequency dominates the pump operating speed. The higher the converter frequency is, the faster the pump runs. High pump operating speed leads to high expander inlet pressure and vice versa. In the shutdown process, the throttle valve pass is used again instead of the expander pass. The expander inlet pressure drops to the expander outlet pressure which is nearly equal to the condensing pressure. In the operating condition, the condensing pressure is about 4.7 MPa and the condensing temperature is in the vicinity of 12.6 °C.

Fig. 6 shows the influence on the mass flow rate of CO_2 by the converter frequency. The variation trend is very similar to the expander inlet pressure. There is a rapid decrease in the start-up and transition process and a sudden drop in the shutdown process. These phenomena are caused by the same reason as the
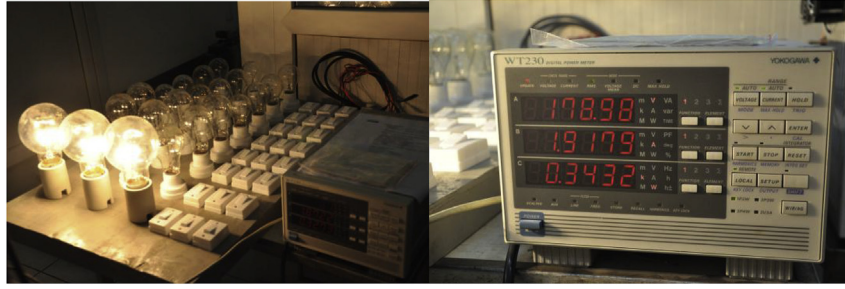
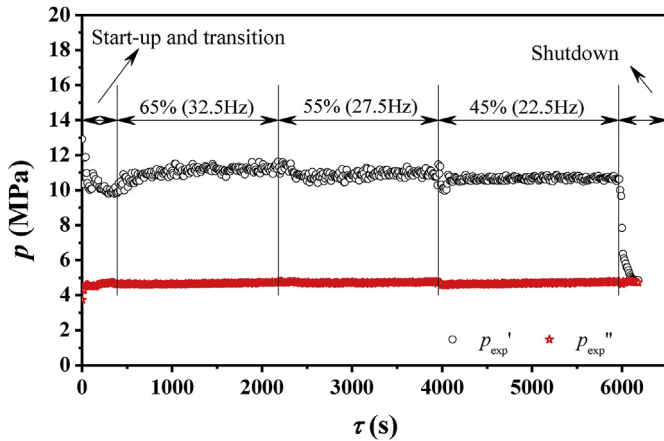**Fig. 4.** The operational aspect of the load bulbs and the power meter.

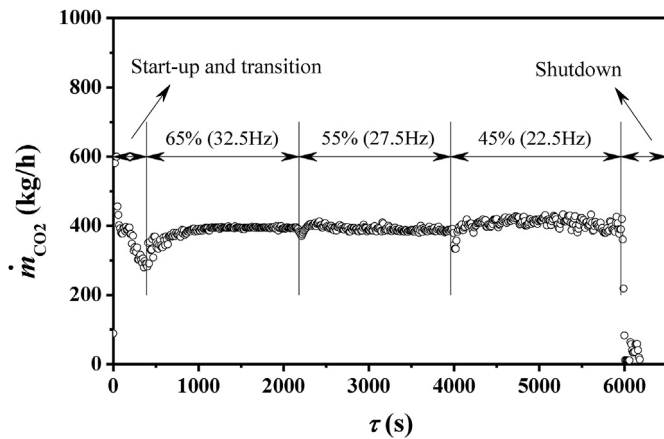**Fig. 5.** Variation of the expander inlet and outlet pressure with time.

Fig. 6. Variation of the CO_2 flow rate with time.

expander inlet pressure. High pressure difference leads to high mass flow rate of working fluid. Therefore, the valve's regulations and the pump's shutdown cause the parameters' rapid decrease in the start-up and transition process and the sudden drop in the shutdown process. In the shutdown process, the converter frequency is regulated from the operating value to low value slowly and the pump is shutdown finally.

An important phenomenon should be noted that mass flow rate of CO_2 with low converter frequency has larger pulse amplitude than that with high converter frequency. However, as shown in Fig. 5, expander inlet pressure with low converter frequency has less pulse amplitude than that with high converter frequency. In

the condition with the converter frequency of 45% (22.5 Hz), the expander inlet pressure is lower than that with higher converter frequency. High expander inlet pressure makes the expander produce great torque and the working fluid flow smoothly and vice versa. As shown in Fig. 4, the system generates more electric power in the conditions with higher converter frequency. Therefore, when the load resistance keeps constant (500 W bulb for each load resistance), the mass flow rate of CO_2 with low converter frequency has larger pulse amplitude than that with high converter frequency.

As shown in Fig. 7, the temperature drop in the expander is about 50 °C. The rolling piston expander is a positive-displacement expansion engine. The pressure drop and the temperature drop depend on the structure design. The little increase of the expander inlet and outlet temperature is caused by the little fluctuation of the thermal oil inlet temperature. In the shutdown process, the temperature increases with slowing down the pump and the mass flow rate of fluid. The temperature drop in shutdown process occurs in the throttle valve.

3.3. Influence of the load resistance

The load resistance has important influence on the performance of the expander and the system. In the stable operating condition of the expander, mechanical power outputted by the expander is equal to the power consumed by the load resistance and the losses. Then the load resistance has great relation with the expander rotational speed and the expander torque [4]. This section gives the influence of the load resistance on the operating parameters. Table 5 shows the connection mode and the load resistance value for the experimental conditions. Two converter frequency values are considered, namely, 35% (17.5 Hz) and 25% (12.5 Hz). The load resistance is regulated by changing the combination and the
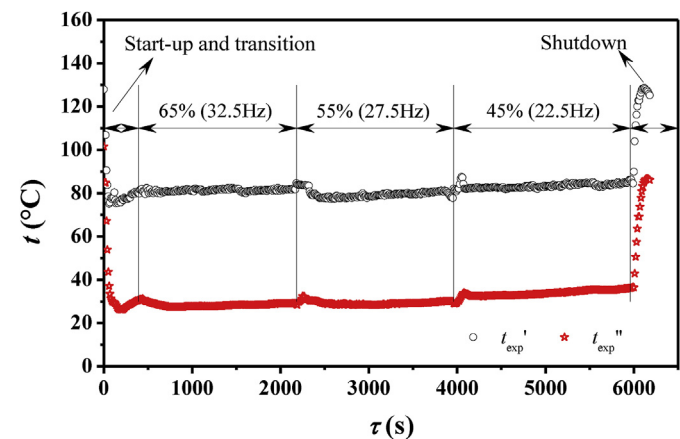

Fig. 7. Variation of the expander inlet and outlet temperature with time.

Table 5
The value of single load resistance used in each condition.

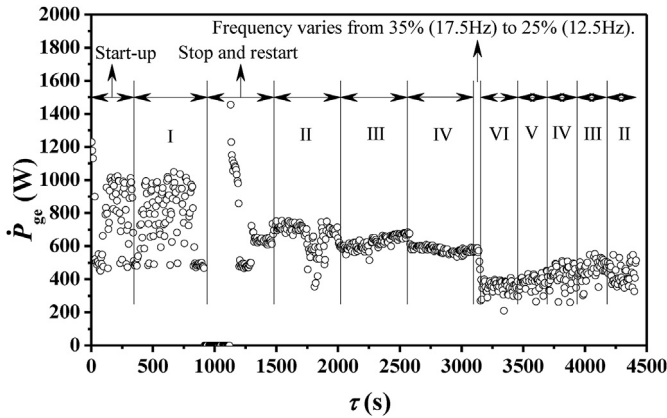| Symbol	Resistance value (Ω)	Connection mode
I	96.8	$Bulb_{500W}$
II	564.7	$Bulb_{200W} + Bulb_{150W}$
III	726.0	$Bulb_{200W} + Bulb_{100W}$
IV	1048.7	$Bulb_{200W} + Bulb_{60W}$
V	2178.0	$Bulb_{200W} + Bulb_{25W}$
VI	4194.7	$Bulb_{150W} + Bulb_{25W} + Bulb_{25W}$

Fig. 8. Variation of the electric power generated with time and the load resistance.
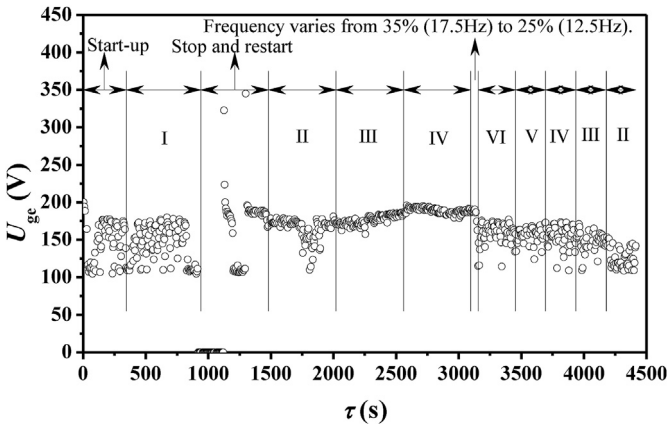

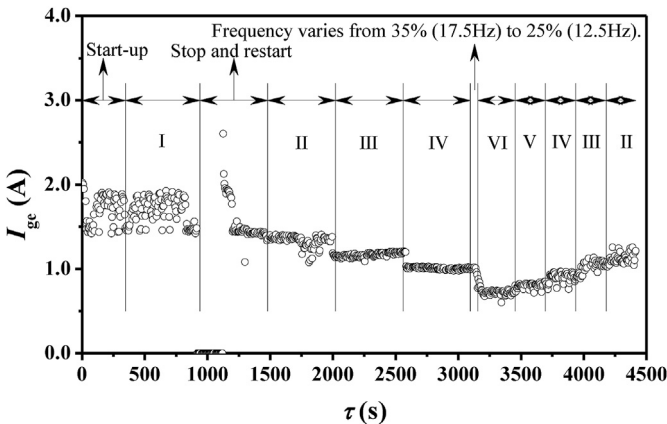**Fig. 9.** Variation of the single load resistance voltage with time.

Fig. 10. Variation of the single load resistance electric current with time.
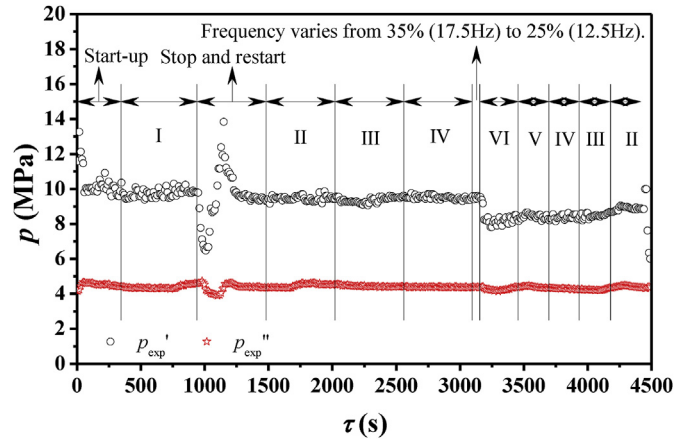

Fig. 11. Variation of the expander inlet and outlet pressure with time and the load resistance.
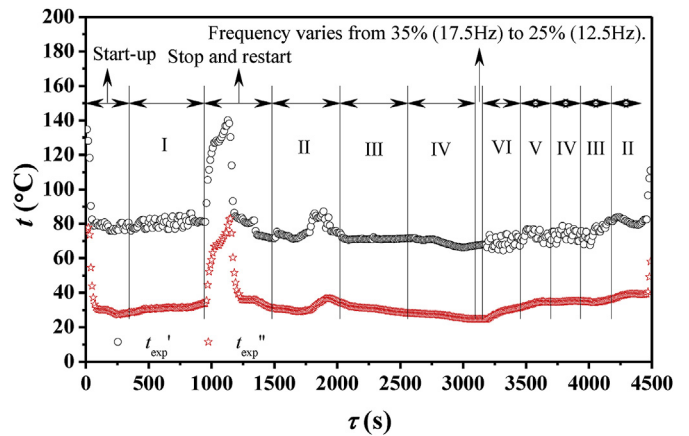

Fig. 12. Variation of the expander inlet and outlet temperature with time and the load resistance.

number of the bulbs. In this section, the inlet temperature of the cooling water keeps about 5 °C and the thermal oil keeps about 210 °C. The condensing temperature is about 10.0 °C while the condensing pressure is about 4.4 MPa.

As shown in Fig. 8, in the start-up process, the electric power generated varies in the range of 400–1100 W, as well as when
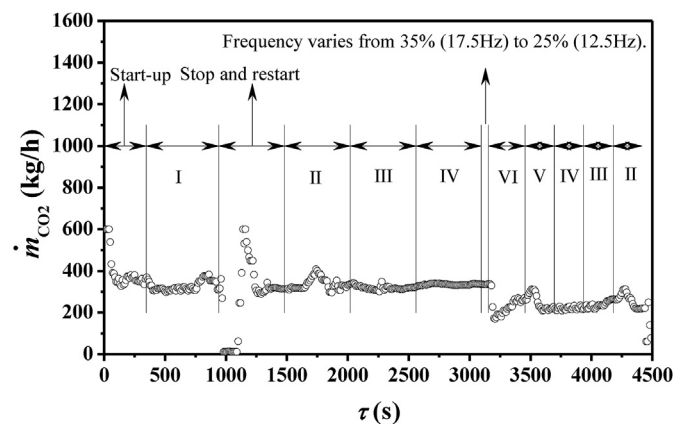

Fig. 13. Variation of the CO_2 flow rate with time and the load resistance.

Table 6
The operating parameters in the considered condition.

$\dot{m}_{CO2}$ kg/h	$\dot{P}_{ge}$ W	t'_{heater} °C	t''_{heater} °C	p'_{heater} MPa	p''_{heater} MPa	t'_{exp} °C	t''_{exp} °C	p'_{exp} MPa	p''_{exp} MPa	η_{ther} %	$\eta_{exp,isen}$ %
395	1115.7	25.4	81.5	11.23	11.18	81.5	27.8	11.18	4.65	5.0	22.0

the converter frequency is 35% (17.5 Hz) and the single load resistance is 96.8 Ω (I: one 500 W bulb). When the converter frequency is 35% (17.5 Hz), the expander outputs little torque while the load is large (low load resistance), thus the expander drives the generator laboriously. This reason causes the violent fluctuation of the electric power and leads to a sudden shutdown of the expander. When each load resistance is 564.7 Ω (II: one 200 W bulb and one 150 W bulb) and 726.0 Ω (III: one 200 W bulb and one 100 W bulb), there is still a little fluctuation. However, it is clearly that there is nearly little fluctuation as the single load resistance is 1048.7 Ω (IV: one 200 W bulb and one 60 W bulb), which indicates that the load matches the operating condition (cycle parameters and expander parameters). To a certain extent, fluctuation exists throughout the considered conditions when the converter frequency is 25% (12.5 Hz), but it still can be observed that the fluctuation with the single load resistance of 4194.7 Ω (VI: one 150 W bulb and two 25 W bulbs) is weaker than the other conditions. If the conditions with different converter frequency are contrasted together, it can be concluded that the electric power value with high converter frequency is smooth with time. The expander can provide high torque with high converter frequency.

Figs. 9 and 10 show the voltage and the electric current for the single load resistance. It is indicated in the two figures that the fluctuation of the electric power is due to the variation of the voltage and the electric current. When the converter frequency keeps constant, the voltage changes a little with changing the load resistance. For the permanent magnet generator, the rotational speed is directly proportional to the voltage. In consideration of the information that the rated rotational speed and the rated voltage are 1000 rpm and 220 V, the generator rotational speed can be achieved from the voltage value that is showed in Fig. 9, as well as the expander rotational speed. The expander rotational speed varies in the range of about 455–910 rpm owing to the voltage in the range of about 100–200 V.

As shown in Fig. 10, the electric current declines obviously with increasing the load resistance, which is different from the voltage. The electric power declines as increasing the resistance, but the expander rotational speed and the generator rotational speed change a little. However, the expander rotational speed and the generator rotational speed display an obvious decrease with decreasing the converter frequency. It is indicated that the electric current and the axis torque have similar variation trend.

Fig. 11 provides the variation of the expander inlet and outlet pressure with time and the load resistance. The load resistance impacts on the match of the expander and the generator rather than the inlet and outlet parameters of the expander. Hence the inlet and outlet parameters of the expander vary a little with changing the load resistance, as shown in Figs. 11 and 12. For positive-displacement expansion engine, the mass flow rate is directly proportional to the expander rotational speed. A conclusion has been obtained from the above analysis that the expander rotational speed varies a little with changing the load resistance while decreases obviously with declining the converter frequency. Consequently, the mass flow rate of the working fluid keeps nearly constant with changing the load resistance while comes down with decreasing the converter frequency, as shown in Fig. 13.

3.4. The thermal efficiency and the expander efficiency

In this section, a condition is selected for analyzing the thermal efficiency and the expander efficiency. The condition is at about 1300 s in Section 3.2. The condensing temperature is about 12.6 °C while the condensing pressure is about 4.7 MPa. The other operating parameters in the considered condition are shown in Table 6. The thermal efficiency can be achieved using the Eq. (1) and the Eq. (2). The result of the thermal efficiency is 5.0%. The isentropic efficiency of the expander can be calculated by the Eq. (3). In the considered condition, the expander isentropic efficiency can reach as much as 21.4%. The performance of the system isn't very good, whereas it still has important significance for the study on the CO_2 transcritical power cycle and the CO_2 expander.

4. Conclusion

This article carries out experimental study on the performance of a CO_2 transcritical power cycle system integrated with a rolling piston expander. The operating parameters and the performance are analyzed.

(1) Due to the start-up mode, a sudden decrease for the electric power generated exists in the process. In the operating process, the electric power rises with increasing the converter frequency.
(2) When the converter frequency keeps constant, for the single load resistance, the electric current declines with increasing the load resistance while the voltage changes a little. Consequently, the electric power generated shows a negative correlation with the load resistance.
(3) Based on a considered condition in which the high pressure is about 11 MPa and low pressure is about 4.6 MPa, the electric power generated can reach 1100 W and the thermal efficiency 5.0%. The isentropic efficiency of about 21.4% is provided by the rolling piston expander also in the above condition.

Nomenclature

M	molar mass (g/mol)
p	pressure (MPa)
t	temperature (°C)
h	enthalpy (kJ/kg)
$\dot{m}$	mass flow rate (kg/s)
$\dot{P}$	power (W)

$\dot{Q}$	heat capacity (W)
U	voltage (V)
I	electric current (A)
LFL	low flame limit (%)
ODP	ozone depression potential
GWP	global warming potential
ORC	organic Rankine cycle
1, 2, 3, 4, 5, a, b	state points of CO_2 transcritical power cycle

Greek letters

| η | efficiency |
| τ | time (s) |

Subscripts

c	critical
b	boiling
cond	condensing
exp	expander
ge	generator
ther	thermal
isen	isentropic

Superscripts

| ′ | inlet |
| ″ | outlet |

References

[1] Tchanche BF, Papadakis G, Lambrinos G, Frangoudakis A. Fluid selection for a low-temperature solar organic Rankine cycle. Appl Therm Eng 2009;29(11–12):2468–76.

[2] Madhawa Hettiarachchi HD, Golubovic M, Worek WM, Ikegami Y. Optimum design criteria for an organic Rankine cycle using low-temperature geothermal heat sources. Energy 2007;32(9):1698–706.

[3] Pan LS, Wang HX. Improved analysis of organic Rankine cycle based on radial flow turbine. Appl Therm Eng 2013;61(2–3):606–15.

[4] Pan LS, Wang HX. Regulation law of turbine and generator in organic Rankine cycle power generation experimental system. Trans Tianjin Univ 2014;20(4): 237–42.

[5] Calm JM, Hourahan GC. Refrigerant data summary update. HPAC Eng 2007;79: 50–64.

[6] Yang L, Yu H, Wang S, Wang H, Zhou Q. Carbon dioxide captured from flue gas by modified Ca-based sorbents in fixed-bed reactor at high temperature. Chin J Chem Eng 2013;21(2):199–204.

[7] Xu D, Xiao P, Li G, Zhang J, Webley P, Zhai Y. CO_2 capture by vacuum swing adsorption using F200 and sorbead WS as protective pre-layers. Chin J Chem Eng 2012;20(5):849–55.

[8] Zhao Z, Dong H, Zhang X. The research progress of CO_2 capture with ionic liquids. Chin J Chem Eng 2012;20(1):120–9.

[9] Guo T, Wang H, Zhang S. Comparative analysis of CO_2-based transcritical Rankine cycle and HFC245fa-based subcritical organic Rankine cycle (ORC) using low-temperature geothermal source. Sci China Technol Sci 2010;53(6): 1869–900.

[10] Chen H, Goswami DY, Rahman MM, Stefanakos EK. Energetic and exergetic analysis of CO_2- and R32-based transcritical Rankine cycles for low-grade heat conversion. Appl Energy 2011;88(8):2802–8.

[11] Garg P, Kumar P, Srinivasan K, Dutta P. Evaluation of carbon dioxide blends with isopentane and propane as working fluids for organic Rankine cycles. Appl Therm Eng 2013;52(2):439–48.

[12] Pan LS, Wang HX, Shi WX. Performance analysis of a zeotropic mixture (R290/ CO_2) for trans-critical power cycle. Chin J Chem Eng 2015;23(3):572–7.

[13] Zhang X, Yamaguchi H, Uneno D. Experimental study on the performance of solar Rankine system using supercritical CO_2. Renew Energy 2007;32(15): 2617–28.

[14] Yamaguchi H, Zhang XR, Fujima K, Enomoto M, Sawada N. Solar energy powered Rankine cycle using supercritical CO_2. Appl Therm Eng 2006;26(17–18):2345–54.

[15] Kim YM, Kim CG, Favrat D. Transcritical or supercritical CO_2 cycles using both low- and high-temperature heat sources. Energy 2012;43(1):402–15.

[16] Batet L, Alvarez-Fernandez JM, Mas de les Valls E, Martinez-Quiroga V, Perez M, Reventos F, et al. Modeling of a supercritical CO_2 power cycle for nuclear fusion reactors using RELAP5-3D. Fusion Eng Des 2014;89(4): 354–9.

[17] Garg P, Srinivasan K, Dutta P. Comparison of CO_2 and steam in transcritical Rankine cycles for concentrated solar power. Energy Procedia 2014;49: 1138–46.

[18] Iverson BD, Conboy TM, Pasch JJ. Supercritical CO_2 Brayton cycles for solar-thermal energy. Appl Energy 2013;111(11):957–70.

[19] Halimi B, Suh KY. Computational analysis of supercritical CO_2 Bragyton cycle power conversion system for fusion reactor. Energy Convers Manag 2012;63(11):38–43.

[20] Lemmon EW, Huber ML, McLinden MO. NIST standard reference database 23, reference fluid thermodynamic and transport properties (REFPROP), version 9.0. National Institute of Standards and Technology; 2010.